Geoacoustic Inversion Based on a Vector Hydrophone Array *

PENG Han-Shu(彭汉书)[1,2], LI Feng-Hua(李风华)[1**]

[1] National Laboratory of Acoustics, Chinese Academy of Sciences, Beijing 100080
[2] Graduate School of the Chinese Academy of Sciences, Beijing 100049

(Received 25 January 2007)

We propose a geoacoustic inversion scheme employing a vector hydrophone array based on the fact that vector hydrophone can provide more acoustic field information than traditional pressure hydrophones. Firstly, the transmission loss of particle velocities is discussed. Secondly, the sediment sound speed is acquired by a matched-field processing (MFP) procedure, which is the optimization in combination of the pressure field and vertical particle velocity field. Finally, the bottom attenuation is estimated from the transmission loss difference between the vertical particle velocity and the pressure. The inversion method based on the vector hydrophone array mainly has two advantages: One is that the MFP method based on vector field can decrease the uncertain estimation of the sediment sound speed. The other is that the objective function based on the transmission loss difference has good sensitivity to the sediment attenuation and the inverted sediment attenuation is independent of source level. The validity of the inverted parameters is examined by comparison of the numerical results with the experimental data.

PACS: 43. 30. Pc, 43. 30. Bp

The purpose of geoacoustic inversion is to estimate the ocean bottom acoustic parameters such as sediment sound speeds, densities, and attenuations from the measured acoustic field. Geoacoustic inversion can give some bottom parameters, which cannot be measured immediately by coring the sediment. Therefore, geoacoustic inversion has attracted much attention in recent years.[1−9] However, there are few related inversion works involving in vector hydrophones. Besides the pressure field, the vector hydrophone can provide the particle velocity directly or indirectly, which can provide more information for geoacoustic inversion. In this Letter, we propose an inversion scheme based on a vector hydrophone array to carry out the geoacoustic inversion.

According to the normal-mode theory, the vector acoustic field excited by a harmonic point source in range-independent shallow water can be expressed by

$$p(r,z) = \frac{i}{\sqrt{8\pi r}} e^{i\pi/4} \sum_l \psi_l(z_s)\psi_l(z) \cdot \frac{1}{\sqrt{\nu_l}} e^{-i\eta_l r} e^{-\beta_l r}, \tag{1a}$$

$$\boldsymbol{v}_r(r,z) = \frac{i}{\rho\omega\sqrt{8\pi r}} e^{i\pi/4} \sum_l \psi_l(z_s)\psi_l(z) \cdot \sqrt{\nu_l} e^{-i\eta_l r} e^{-\beta_l r}, \tag{1b}$$

$$\boldsymbol{v}_z(r,z) = \frac{1}{\rho\omega\sqrt{8\pi r}} e^{i\pi/4} \sum_l \psi_l(z_s)\psi_l'(z) \cdot \nu_l^{-1/2} e^{-i\eta_l r} e^{-\beta_l r}, \tag{1c}$$

where $\nu_l = \eta_l + \beta_l$ is the complex eigenvalue of the modes, the real part η_l of the eigenvalue is the horizontal wavenumber, and the imaginary part β_l of the eigenvalue is the normal mode attenuation, $\psi_l(z)$ is the eigenfunction, and $\psi_l'(z) = (\partial/\partial_z)\psi_l(z)$, z and z_s are the depths of receiver and source, respectively.

Referring to the definition of transmission loss, we define the vector transmission loss as

$$TL_p = -20\lg\Big|\frac{p(r,z)}{p_0(r=1)}\Big|, \tag{2a}$$

$$TL_{\boldsymbol{v}}^r = -20\lg\Big|\frac{\boldsymbol{v}_r(r,z)}{\boldsymbol{v}_{r0}(r=1)}\Big|, \tag{2b}$$

$$TL_{\boldsymbol{v}}^z = -20\lg\Big|\frac{\boldsymbol{v}_z(r,z)}{\boldsymbol{v}_{r0}(r=1)}\Big|, \tag{2c}$$

where the reference pressure $p_0(r) = e^{ikr}/4\pi r$, and the reference particle velocity $\boldsymbol{v}_{r0}(r) = -\frac{1}{i\rho\omega}\frac{\partial p_0(r)}{\partial r} = \frac{1}{i\rho\omega}\frac{e^{ikr}}{4\pi r}\left(\frac{1}{r} - ik\right)$, TL_p, $TL_{\boldsymbol{v}}^r$ and $TL_{\boldsymbol{v}}^z$ represent the transmission loss of the pressure, the horizontal particle velocity and the vertical particle velocity, respectively, and $k = \omega/c(z_s)$ with ω being the angular frequency of sound.

According to the normal-mode theory, the high-order normal modes will contribute more to the vertical particle velocity due to their large grazing angle; on the other hand, the low-order normal modes will contribute more to the pressure and the horizontal particle velocity. Thus the vertical particle velocity field is composed of a larger proportion of high-order normal mode in comparison with the pressure field and the horizontal particle velocity field in most cases. Because of the rapid attenuation of high-order normal mode by the sea bottom, the vertical particle velocity will decrease relatively rapidly.

An experiment involving vector hydrophones was conducted in the Yellow Sea in September 2006. Fig-

* Supported by the National Natural Science Foundation of China under Grand No 10574136.
** To whom correspondence should be addressed. Email: lfh@mail.ioa.ac.cn
©2007 Chinese Physical Society and IOP Publishing Ltd

ure 1 shows the experimental configuration. Four vector hydrophones, one of which has four channels of x, y, z and p, were used to form a vertical array at the receiving ship in this experiment. At the same time, along the shipping track of the transmitting ship, explosive sources were exploded. Figure 2 shows the signal received by the vector hydrophone 2 with depth of 29.32 m at the distance of 18 km from the source, where the central frequency is 400 Hz with 1/3 Oct band. In Fig. 2, channels x and y provides the two components of the horizontal particle velocity, channel z provides the vertical particle velocity, and signal p provides the pressure.

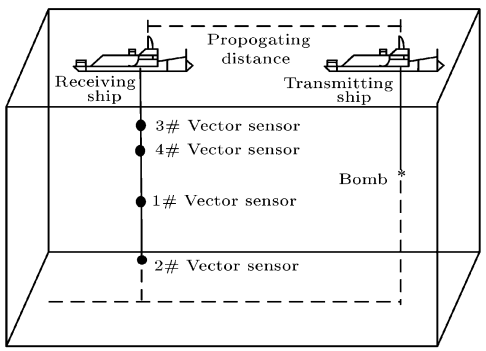

Fig. 1. Experiment model.

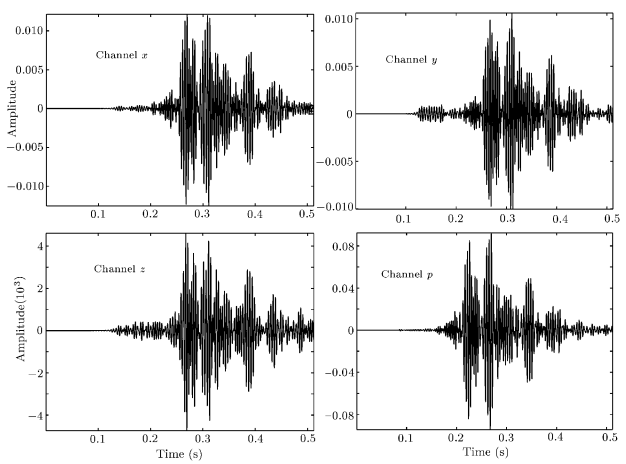

Fig. 2. Vector experimental signal.

With the signal received by channels x, y, z and p, we can obtain the experimental data of the transmission loss as shown in Fig. 3, in which asterisks, triangles and circles represent the transmission loss of the horizontal particle velocity, the vertical particle velocity and the pressure respectively. The corresponding theoretical results are also given in the figure. It can be seen from the figure that the attenuation of the horizontal particle velocity is similar to the pressure and the vertical particle velocity decreases rapidly, which is in agreement with the vector characteristic described above. Thus either from the theoretical results or the experimental data we can draw the conclusion that the attenuation of vertical particle velocity will decrease rapidly in comparison with the pressure and the horizontal velocity in shallow water. This will be used to invert the sediment attenuation in this study.

A half-infinite liquid bottom model with three parameters, i.e. density ρ_b, sound speed c_b and attenuation α_b, is used in our geoacoustic inversion scheme. Discussions in Refs. [3,4] have already shown that this equivalent seabed model has the same acoustic effect on the underwater sound field as the multiple-layer models within some range-frequency domain of interest. In this Letter, we obtain the density $\rho_b = 1.78\,\mathrm{g/cm^3}$ from the sediment coring of the adjacent area in an experiment conducted in 2002,[5] then the main interest of this study will focus on the inversion of sound speed and attenuation. What is more, the measuring error of sea depth h_b has been proven to affect the geoacoustic inversion obviously,[1] the sea depth will be inverted. Due to different sensitivities to the sediment parameters, different methods are combined.

One of the most widely used inversion methods, i.e. the matched-field processing (MFP) method, has been proven to be effective to invert the sound speed. However, the previous related works all is focused on the matching of acoustic pressure field. For the vector hydrophone can provide the particle velocity field besides the pressure field, the MFP method based on vector field is provided here to invert the sound speed and the sea depth. Using the multi-frequency incoherent Bartlett processor, the objective functions $E_p(c_b, h_b)$ and $E_{vz}(c_b, h_b)$, which are based on the pressure field and the vertical particle velocity field respectively, are defined as follows:

$$E_p(c_b, h_b) = \frac{1}{M_f} \cdot \sum_{j=1}^{M_f} \left(\frac{\left| \sum_{i=1}^{N} p_i^e(f_j) * p_i^c(f_j, c_b, h_b) \right|^2}{\left[\sum_{i=1}^{N} |p_i^e(f_j)|^2 \right] \left[\sum_{i=1}^{N} |p + i^c(f_j, c_b, h_b)|^2 \right]} \right), \tag{3a}$$

$$E_{\boldsymbol{v}_z}(c_b, h_b) = \frac{1}{M_f} \cdot \sum_{j=1}^{M_f} \left(\frac{\left| \sum_{i=1}^{N} \boldsymbol{v}_{zi}^e(f_j) * \boldsymbol{v}_{zi}^c(f_j, c_b, h_b) \right|^2}{\left[\sum_{i=1}^{N} |\boldsymbol{v}_{zi}^e(f_j)|^2 \right] \left[\sum_{i=1}^{N} |\boldsymbol{v}_{zi}^c(f_j, c_b, h_b)|^2 \right]} \right), \tag{3b}$$

where $p_i^e(f)$ and $\boldsymbol{v}_{zi}^e(f)$ are the experimental complex pressure field and vertical particle velocity field received by the ith vector hydrophone, $p_i^c(f)$ and $\boldsymbol{v}_{zi}^c(f)$ are the theoretically predicted pressure field and vertical particle velocity field, respectively, N is the hydrophone number of the vector array, superscript $*$ represents the complex conjugation, j is the frequency

index, and M_f is the number of frequency. Here, only c_b and h_b are inverted; this is reasonable because the attenuation is relatively less sensitive to the MFP inversion. The two objective functions $E_p(c_b, h_b)$ and $E_{\boldsymbol{v}z}(c_b, h_b)$ will show different sensitivities to the same combination of c_b and h_b. To reach the optimal matching of the true acoustic field, the final objective function $E(c_b, h_b)$ is chosen as Eq. (4), which is based on the vector field,

$$E(c_b, h_b) = \sqrt{E_p(c_b, h_b) \cdot E_{v_z}(c_b, h_b)}. \tag{4}$$

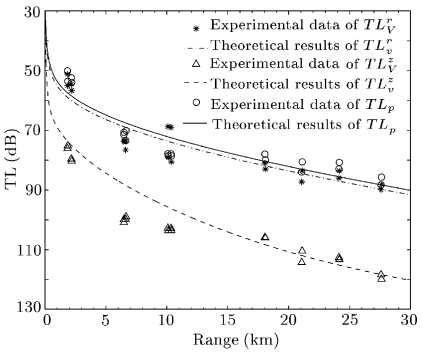

Fig. 3. Vector transmission loss.

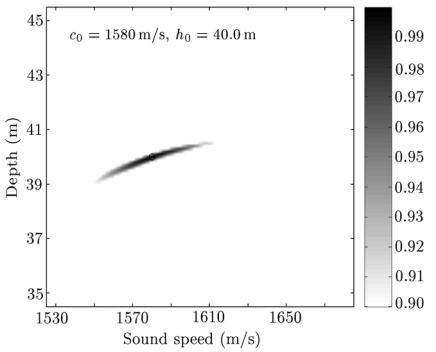

Fig. 4. Simulation of the objective function with the MFP by pressure field.

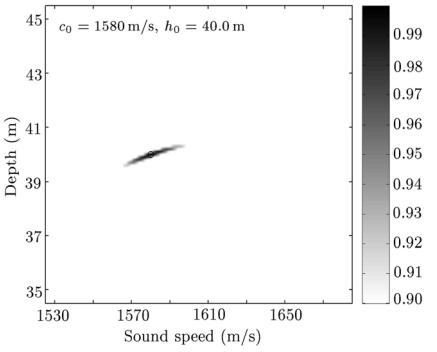

Fig. 5. Simulation of the objective function with the MFP by vector field.

To show the advantage of the MFP method based on the vector field more clearly, the simulated results of $E_p(c_b, h_b)$ and $E(c_b, h_b)$ are illustrated in Figs. 4 and 5, respectively. The ground truth of the bottom sound speed and sea depth are $c_0 = 1580$ m/s and $h_0 = 40$ m. The frequency band is 200–300 Hz and the hydrological condition is the same as Fig. 1. If we assume that the uncertain estimation of the inversion is the value (0.9–1.0) of the objective function, by the MFP method based on the pressure field, the possible scope of sound speed is about ± 30 m/s; while by the MFP method based on the vector field, the corresponding scope is about ± 10 m/s. Then the MFP methods based on pressure field and vector field are applied to this experiment, the results are shown in Figs. 6 and 7, respectively. If we assume that the uncertain estimation of the inversion is the value of the objective function, in the range of 0.05 from the maximum, it can also be seen that the side lobe of the objective function by the vector field will reduce greatly in comparison with that by the pressure field. Thus from either the simulative results or the experimental data we can conclude that the MFP method based on the vector field can reduce the side lobe of the objective function, which can decrease the uncertain estimation of the inversion. A physical interpretation is that pressure can provide more horizontal field information for its high proportion of low-order normal mode, while vertical velocity can provide more vertical field information for its high proportion of high-order normal mode. Thus the combination of them can provide more detailed field information for the matching. Finally, from Fig. 7 we obtain the estimation result of $c_b = 1582$ m/s and $h_b = 40.2$ m.

Since the density and the sound speed have been obtained, the only unknown bottom parameter is the attenuation coefficient. The transmission loss difference between the vertical particle velocity and the pressure, $\Delta_{TL} = TL_{\boldsymbol{v}}^z - TL_p$, is used to invert the attenuation coefficients. Since Δ_{TL} is obtained by subtracting the pressure transmission loss from the vertical particle velocity transmission loss directly with the same explosive source, the attenuation inversion by vector sensor is independent of source level, thus the fluctuate of source level (especially for explosive source) can be avoided. The standard deviation of Δ_{TL} is used as the cost function:

$$\varepsilon(\alpha_b) = \sqrt{\Big(\sum_{i=1}^{Nr}[\Delta_{TL}^c(\alpha_b, r_i) - \Delta_{TL}^e(r_i)]^2\Big)\Big/(N_r - 1)} \tag{5}$$

where Δ_{TL}^c and Δ_{TL}^e represent the theoretical and the experimental Δ_{TL} respectively, r_i is the transmission distance, N_r is the number of the distances taken in the calculation.

The relationship of ε versus α_b is shown in Fig. 8, where the frequency is 400 Hz. It can be seen that the objective function has good sensibility to the bottom attenuation. Then at the minimum of ε, we can obtain $\alpha_b = 0.058$ dB/m. Following this, the inverted bottom attenuations in the frequency range of 100–1000 Hz are depicted in Fig. 9. Fitting the data yields

$$\alpha = 0.479 f^{0.81}(\mathrm{dB}/\lambda), \text{ or } \alpha = 0.303 f^{1.81}(\mathrm{dB/m}), \tag{6}$$

where frequency f is in units of kHz. It can be seen that in the frequency range of 100–1000 Hz, the inverted bottom attenuation has nonlinear frequency dependence. This is coincident with the conclusions described in Refs. [1,5–7]. The equivalent bottom attenuations often exhibit nonlinear frequency dependence in the low frequency range.

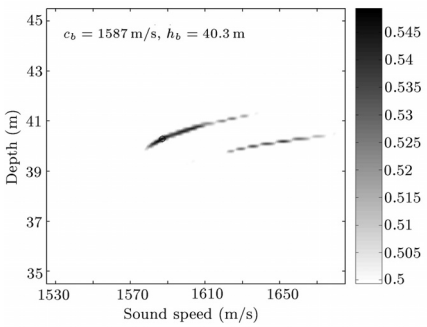

Fig. 6. Experimental result of the objective function with the MFP by pressure field.

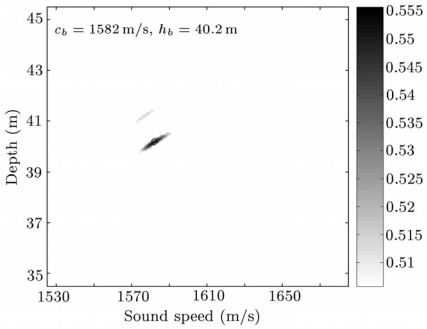

Fig. 7. Experimental result of the objective function with the MFP by vector field.

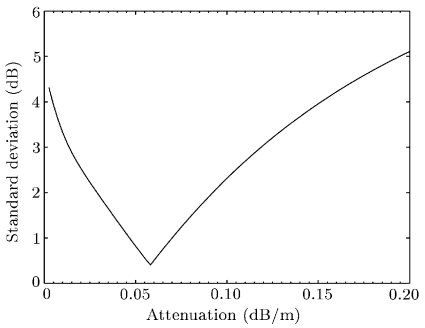

Fig. 8. Standard deviation of Δ_{TL} as a function of α_b.

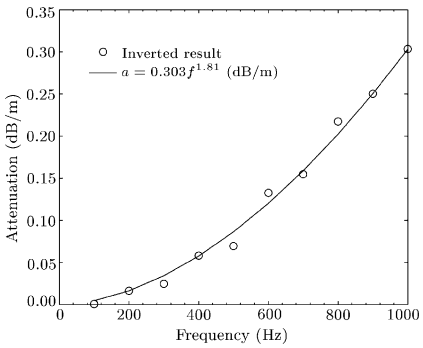

Fig. 9. Inverted attenuation as a function of frequency.

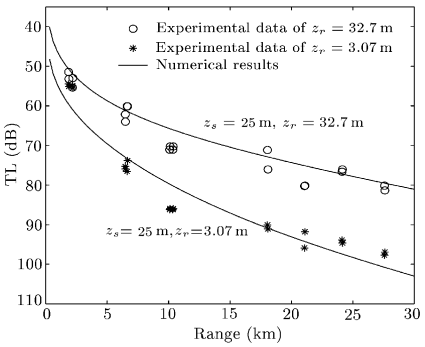

Fig. 10. Transmission loss with different receiver depths z_r and with the same source depth $z_s = 25$ m.

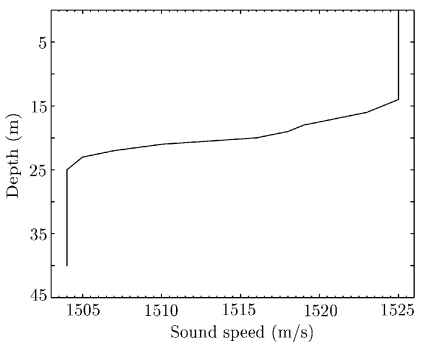

Fig. 11. Sound speed profile.

Figure 10 shows the comparisons of the measured transmission loss by another vertical array composed of pressure sensors used in this experiment and the numerical transmission loss calculated with the inverted bottom parameters. The central frequency is 400 Hz with 1/3 Oct band. z_s and z_r are the depths of the source and the receiver, respectively. The two receivers are above and below the thermocline (the sound speed profile is shown in Fig. 11) with depths of 3.07 m and 32.7 m, and the experimental data of them are signed by asterisks and circles, respectively. It is shown from Fig. 10 that the numerical TL is in good agreement with the experimental data.

In summary, we have proposed a new geoacoustic inversion scheme based on the experimental data measured by the vector hydrophone array. This inversion scheme can make use of the more detailed field information provided by a vector hydrophone. It mainly has the following two advantages: One is that the MFP method based on the vector field can decrease the uncertain estimation of the sediment sound speed. The other is that the objective function based on the transmission loss difference has good sensitivity to the sediment attenuation and the inverted sediment attenuation is independent of source level. The validity of the inversion scheme is verified in a sea experiment. The inverted bottom parameters can be used to predict the sound propagations in shallow sea.

All the experimental data used in this study are collected from the Yellow Sea Experiment conducted in September 2006. The authors would like to thank all the participants of the experiment from the National Laboratory of Acoustics and Beihai Branch of Institute of Acoustics, CAS. We would also like to show our appreciation to the professional and competent efforts of the manager (J. Yu), captains, and crew of R/Vs *Kexue* 1 and *Kexue* 3 from the Oceanology Institute of CAS.

We thank Zhang R H for his guidance to the authors.

References

[1] Li F H and Zhang R H 2000 *Acta Acoust.* **25** 298 (in Chinese)
[2] Liu J J, Li F H and Peng Z H 2003 *Chin. Phys. Lett.* **20** 2188
[3] Zhang R H, Li F H and Luo W Y 1998 *J. Comput. Acoust.* **6** 245
[4] Taroudakis M I and Makrakis G N 2001 *Inverse Problems in Underwater Acoustics* (New York: Springer) p 1
[5] Li Z L and Zhang R H 2004 *Chin. Phys. Lett.* **21** 1100
[6] Li Z L, Yan J and Li F H et al 2003 *Chin. J. Acoust.* **22** 176
[7] Zhou J X, Zhang X Z and Rogers P H 1987 *J. Acoust. Soc. Am.* **82** 287
[8] Rajan S D, Lynch J F and Frisk G V 1987 *J. Acoust. Soc. Am.* **82** 998
[9] Potty G R, Miller J H and Lynch J F et al 2000 *J. Acoust. Soc. Am.* **108** 973